Yu. A. Kruglyak

Department of Information Technologies, Odessa State Environmental University, 15, Lvivska Str., Odessa, 65016, Ukraine

Yu. A. Kruglyak

ELECTRIC CURRENT, THERMOCURRENT, AND HEAT FLUX IN NANO- AND MICROELECTRONICS: SELECTED TOPICS

The modern Landauer – Datta – Lundstrom (LDL) electron and heat transport model was briefly summarized in [1], namely: if a band structure is chosen analytically or numerically, the number of conduction modes can be evaluated and, if a model for a mean-free-path for backscattering can be established, then the near-equilibrium thermoelectric transport coefficients can be calculated for 1D, 2D, and 3D resistors of any size in ballistic, quasi-ballistic, and diffusive linear response regimes when there are differences in both voltage and temperature across the device.

The following topics are discussed now in the LDL approach: bipolar conductivity, thermal conductivity of the bulk conductors, specific heat versus thermal conductivity, Debye model, phonon scattering, lattice thermal conductivity versus temperature, difference between lattice thermal and electrical conductivities, lattice thermal conductivity quantization.

Appendices give final expressions of thermoelectric transport coefficients through the Fermi – Dirac integrals for 1D, 2D, and 3D resistors with parabolic band structure and for 2D graphene linear dispersion in ballistic and diffusive regimes with the power law scattering.

Keywords: nanoelectronics, microelectronics, bipolar conductivity, thermal conductivity, Debye model, near-equilibrium transport, phonon scattering, thermal conductivity quantization, thermoelectric transport coefficients.

Introduction

The modern Landauer – Datta – Lundstrom (LDL) electron and heat transport model was briefly summarized in [1]. The LDL model is based on three concepts: conductivity modes $M(E)$, transmission coefficients $T(E)$, Fermi conductivity windows for electrons $(-\partial f_0/\partial E)$ and corresponding expression for phonons proportional to $(-\partial n_0/\partial E)$, where $f_0(E)$ and $n_0(E)$ are Fermi and Bose functions. These window functions are responsible for selecting those electron and phonon conduction modes which only contribute to the electric current and heat flow under the low bias conditions.

The following topics are discussed in the LDL approach below: bipolar conductivity, thermal conductivity of the bulk conductors, specific heat versus thermal conductivity, Debye model, phonon scattering, temperature dependence of the lattice thermal conductivity, difference between lattice thermal and electrical conductivities, lattice thermal conductivity quantization.

In summary, given a band structure dispersion, the number of modes can be evaluated and, if a model for a mean-free-path for backscattering $\lambda(E)$ can be established, then the near-equilibrium transport

coefficients can be calculated using final expressions listed in Appendices where we collect practically useful final expressions for thermoelectric transport coefficients through the Fermi – Dirac integrals for 1D, 2D, and 3D resistors with parabolic band structure and for 2D graphene linear dispersion case in ballistic and diffusive regimes with the power law scattering.

1. Bipolar conduction

Let us consider a 3D semiconductor with parabolic dispersion. For the conduction band

$$M_{3D}^{(c)}(E) = g_v \frac{m_n^*}{2\pi\hbar^2}(E - E_C) \quad (E \geq E_C) \tag{1a}$$

and for the valence band

$$M_{3D}^{(v)}(E) = g_v \frac{m_p^*}{2\pi\hbar^2}(E_V - E) \quad (E \leq E_V)\,. \tag{1b}$$

The conductivity [1] is provided with two contributions: for the conduction band

$$\sigma_n = \frac{q^2}{h}\int\limits_{E_C}^{\infty} M_{3D}^{(c)}(E)\lambda_n(E)\left(-\frac{\partial f_0}{\partial E}\right)dE \tag{2a}$$

and for the valence band

$$\sigma_p = \frac{q^2}{h}\int\limits_{-\infty}^{E_V} M_{3D}^{(v)}(E)\lambda_p(E)\left(-\frac{\partial f_0}{\partial E}\right)dE\,. \tag{2b}$$

The Seebeck coefficient S_n for electrons in the conduction band follows from eqs (66) in [1]:

$$\sigma_n = \int\limits_{E_C}^{\infty} \sigma_n'(E)dE\,, \tag{3a}$$

$$\sigma_n'(E) = \frac{2q^2}{h} M_{3D}^{(c)}(E - E_C)\lambda_n(E)\left(-\frac{\partial f_0}{\partial E}\right), \tag{3b}$$

$$s_T^{(c)} = -\frac{k}{q}\int\limits_{E_C}^{\infty}\left(\frac{E - E_F}{kT}\right)\sigma_n'(E)\,dE\,, \tag{3c}$$

$$S_n = s_T^{(c)} / \sigma_n\,. \tag{3d}$$

Similarly, S_p for electrons in the valence band we have:

$$\sigma_p = \int\limits_{-\infty}^{E_V} \sigma_p'(E)dE\,, \tag{4a}$$

$$\sigma'_p(E) = \frac{2q^2}{h} M_{3D}^{(v)}(E_V - E)\lambda_p(E)\left(-\frac{\partial f_0}{\partial E}\right), \tag{4b}$$

$$s_T^{(v)} = -\frac{k}{q}\int_{-\infty}^{E_V}\left(\frac{E - E_F}{kT}\right)\sigma'_p(E)\,dE, \tag{4c}$$

$$S_p = s_T^{(v)} / \sigma_p, \tag{4d}$$

but the sign of S_p will be positive.

What is going on when both the conduction and valence bands contribute to conduction? This can happen for a narrow bandgap conductors or at high temperatures. In such a case, we have to simply integrate over all the modes and will find

$$\sigma^{tot} \equiv \sigma_n + \sigma_p = \frac{q^2}{h}\int_{E_1}^{E_2} M_{3D}^{tot}(E)\lambda(E)\left(-\frac{\partial f_0}{\partial E}\right)dE, \tag{5a}$$

$$M_{3D}^{tot}(E) = M_{3D}^{(c)}(E) + M_{3D}^{(v)}(E). \tag{5b}$$

Moreover, we have not be worried about integrating to the top of the conduction band or from the bottom of the valence band because the Fermi function ensures that the integrand falls exponentially to zero away from the band edge. What is important that in both cases we integrate the same expression with the appropriate $M_{3D}(E)$ and $\lambda(E)$ over the relevant energy difference $E_2 - E_1$. Electrons carry current in both bands. Our general expression is the same for the conduction and valence bands. There is no need to change signs for the valence band or to replace $f_0(E)$ with $1 - f_0(E)$.

To calculate the Seebeck coefficient when both bands contribute let us remind that in the first direct form of the transport coefficients (66) of [1] the contributions from each mode are added in parallel so the total specific Soret coefficient

$$s_T^{tot} = -\frac{k}{q}\int_{-\infty}^{+\infty}\left(\frac{E - E_F}{kT}\right)\sigma'(E)dE = S_n\sigma_n + S_p\sigma_p; \tag{6a}$$

then the Seebeck coefficient for bipolar conduction

$$S^{tot} = \frac{S_n\sigma_n + S_p\sigma_p}{\sigma_n + \sigma_p}. \tag{6b}$$

Since the Seebeck coefficients for the conduction and valence bands have opposite signs the total Seebeck coefficient just drops for high temperatures and the performance of a thermoelectrical device falls down.

2. Thermal conductivity of the bulk conductors

The thermal conductivity of a large diffusive resistor is a key material property that controls

performance of any electronic devices. By analogy with the transmission coefficient (39) in [1] for electron transport the phonon transmission

$$T_{ph}(\hbar\omega) = \frac{\lambda_{ph}(\hbar\omega)}{\lambda_{ph}(\hbar\omega) + L}\Big|_{L \gg \lambda_{ph}} \to \frac{\lambda_{ph}(\hbar\omega)}{L}. \tag{7}$$

It is also obvious that for large 3D conductors the number of phonon modes is proportional to the cross-sectional area of the sample:

$$M_{ph}(\hbar\omega) \propto A, \tag{8}$$

Now let us return to eqn (76) of [1] dividing and multiplying it by *A/L*, which immediately gives eqn (69) over there for the phonon heat flux postulated in [1]

$$\frac{Q}{A} \equiv J_{Qx}^{ph} = -\kappa_L \frac{dT}{dx} \tag{9}$$

with specific lattice thermal conductivity

$$\kappa_L = K_L \frac{L}{A}, \tag{10}$$

or substituting (7) above to (82) of [1] one for the lattice thermal conductivity finally obtains

$$\kappa_L = \frac{\pi^2 k^2 T}{3h} \int \frac{M_{ph}(\hbar\omega)}{A} \lambda_{ph}(\hbar\omega) W_{ph}(\hbar\omega)\, d(\hbar\omega). \tag{11}$$

It is useful now to define the average number of phonon modes per cross-sectional area of the conductor that participate in the heat transport

$$\left\langle M_{ph} / A \right\rangle \equiv \int \frac{M_{ph}(\hbar\omega)}{A} W_{ph}(\hbar\omega)\, d(\hbar\omega). \tag{12}$$

Then

$$\kappa_L = \frac{\pi^2 k^2 T}{3h} \left\langle M_{ph} / A \right\rangle \left\langle \left\langle \lambda_{ph} \right\rangle \right\rangle, \tag{13}$$

where the average mean-free-path is defined now as

$$\left\langle \left\langle \lambda_{ph} \right\rangle \right\rangle = \frac{\int \frac{M_{ph}(\hbar\omega)}{A} \lambda_{ph}(\hbar\omega) W_{ph}(\hbar\omega)\, d(\hbar\omega)}{\int \frac{M_{ph}(\hbar\omega)}{A} W_{ph}(\hbar\omega)\, d(\hbar\omega)}. \tag{14}$$

Thus, the couple of the phonon transport equations (9) and (13) corresponds to similar electron transport equations:

$$J_x = \frac{\sigma}{q} \frac{d\left(E_F\right)}{dx}, \tag{15}$$

$$\sigma = \frac{2q^2}{h}\langle M_{el} / A\rangle\langle\langle \lambda_{el} \rangle\rangle . \tag{16}$$

The thermal conductivity (13) and the electrical conductivity (16) have the same structure. It is always a product of the corresponding quantum of conductance times the number of modes that participate in transport, times the average mean-free-path. These three quantities for phonons will be discussed later.

3. Specific heat versus thermal conductivity

The connection between the lattice specific thermal conductivity and the lattice specific heat at constant volume is well known [2 – 5]. We will show now that corresponding proportionality coefficient is a product of an appropriately-defined mean-free-path $\langle\langle \Lambda_{ph} \rangle\rangle$ and an average phonon velocity $\langle v_{ph} \rangle$, namely:

$$\kappa_L = \frac{1}{3}\langle\langle \Lambda_{ph} \rangle\rangle\langle v_{ph} \rangle C_V . \tag{17}$$

The total phonon energy per unit volume

$$E_{ph} = \int_0^\infty (\hbar\omega) D_{ph}(\hbar\omega) n_0(\hbar\omega) d(\hbar\omega) , \tag{18}$$

where $D_{ph}(\hbar\omega)$ is the phonon density of states. By definition,

$$\begin{aligned} C_V \equiv \frac{\partial E_{ph}}{\partial T} = \frac{\partial}{\partial T}\int_0^\infty (\hbar\omega) D_{ph}(\hbar\omega) n_0(\hbar\omega) d(\hbar\omega) = \\ = \int_0^\infty (\hbar\omega) D_{ph}(\hbar\omega)\left(\frac{\partial n_0(\hbar\omega)}{\partial T}\right) d(\hbar\omega) = \frac{\pi^2 k^2 T}{3}\int_0^\infty D_{ph}(\hbar\omega) W_{ph}(\hbar\omega) d(\hbar\omega) \end{aligned} . \tag{19}$$

where eqs (74) and (81) of [1] were used. Next, multiply and divide (11) by (19) and obtain proportionality we are looking for:

$$\kappa_L = \left[\frac{\frac{1}{h}\int_0^\infty \frac{M_{ph}(\hbar\omega)}{A}\lambda_{ph}(\hbar\omega) W_{ph}(\hbar\omega) d(\hbar\omega)}{\int_0^\infty D_{ph}(\hbar\omega) W_{ph}(\hbar\omega) d(\hbar\omega)}\right] C_V . \tag{20}$$

To obtain final expression (17) and correct interpretation of the proportionality coefficient we need to return to eqn (7). This expression can be easily derived for 1D conductor with several simplifying assumptions. Nevertheless it works very well in practice for a conductor of any dimension. Derivation of eqn (7) is based on the interpretation of the mean-free-path $\lambda(E)$ or $\lambda(\hbar\omega)$ as that its inverse is the probability per unit length that a positive flux is converted to a negative flux. This is why λ is often called a mean-free-path for backscattering. Let us relate it to

the scattering time τ. The distinction between mean-free-path and mean-free-path for backscattering is easiest to see for 1D conductor. Let electron undergoes a scattering event. For isotropic scattering the electron can forward scatter or back scatter. Only backscattering is relevant for the mean-free-path for scattering, so the time between backscattering events is 2τ. Thus the mean-free-path for backscattering is twice the mean-free-path for scattering

$$\lambda_{1D}(E) = 2\Lambda(E) = 2v(E)\tau(E). \tag{21a}$$

It was shown that the proper definition of the mean-free-path for backscattering for a conductor of any dimension [6]

$$\lambda(E) = 2\frac{\langle v_x^2\tau\rangle}{\langle|v_x|\rangle},$$

where averaging is performed over angles. For isotropic bands

$$\lambda_{2D}(E) = \frac{\pi}{2}v(E)\tau(E), \tag{21b}$$

$$\lambda_{3D}(E) = \frac{4}{3}v(E)\tau(E). \tag{21c}$$

The scattering time is often approximately written as the power law scattering

$$\tau(E) = \tau_0\left(\frac{E-E_C}{kT}\right)^s, \tag{22}$$

where exponent *s* describes the specific scattering mechanism: for acoustic phonon scattering in 3D conductor with parabolic dispersion $s=-1/2$, and for ionized impurity scattering $s=+3/2$ [7].

Analogous power law is often used for mean-free-path:

$$\lambda(E) = \lambda_0\left(\frac{E-E_C}{kT}\right)^r. \tag{23}$$

For parabolic zone structure $v(E)\propto E^{1/2}$, thus $r=s+1/2$ with $r=0$ for acoustic phonon scattering, and $r=2$ for ionized impurity scattering.

Coming back to our initial task to derive (17) from (20) for 3D conductor according (21c) we have

$$\lambda_{ph}(\hbar\omega) = \frac{4}{3}v_{ph}(\hbar\omega)\tau_{ph}(\hbar\omega), \tag{24}$$

where according to (21a),

$$v_{ph}(\hbar\omega)\tau_{ph}(\hbar\omega) = \Lambda_{ph}(\hbar\omega), \tag{25}$$

and finally

$$\lambda_{ph}(\hbar\omega) = \frac{4}{3}\Lambda_{ph}(\hbar\omega)\,. \tag{26}$$

It was stated above in (18) of [1] that the density of states and number of modes for electrons in 3D:

$$M_{el}(E) = AM_{3D}(E) = A\frac{h}{4}\left\langle v_x^+(E)\right\rangle D_{3D}(E)\,. \tag{27}$$

Let us rewrite this formulae for phonons. Note that the spin degeneracy for electrons $g_S = 2$ is included to the density of states

$$D_{3D}(E) = 2D'_{3D}(E)\,, \tag{28}$$

and for spherical bands in 3D conductor

$$\left\langle v_x^+(E)\right\rangle = \frac{v_{el}(E)}{2}\,. \tag{29}$$

Collecting (27) up to (29) all together in case of phonons we have

$$M_{ph}(\hbar\omega) = A\frac{h}{2}\left(\frac{v_{ph}(\hbar\omega)}{2}\right)2D_{ph}(\hbar\omega) = A\frac{h}{4}v_{ph}(\hbar\omega)D_{ph}(\hbar\omega)\,. \tag{30}$$

Substituting (26) and (30) to (20) we obtain

$$\kappa_L = \left[\frac{\frac{1}{3}\int_0^\infty \Lambda_{ph}(\hbar\omega)v_{ph}(\hbar\omega)D_{ph}(\hbar\omega)W_{ph}(\hbar\omega)d(\hbar\omega)}{\int_0^\infty D_{ph}(\hbar\omega)W_{ph}(\hbar\omega)d(\hbar\omega)}\right]C_V\,. \tag{31}$$

Multiplying and dividing (31) by

$$\int_0^\infty v_{ph}(\hbar\omega)D_{ph}(\hbar\omega)W_{ph}(\hbar\omega)d(\hbar\omega)\,, \tag{32}$$

we finally get eqn (17) with proportionality coefficient between κ_L and C_V as the product of an average mean-free-path as

$$\left\langle\left\langle\Lambda_{ph}\right\rangle\right\rangle \equiv \frac{\int_0^\infty \Lambda_{ph}(\hbar\omega)v_{ph}(\hbar\omega)D_{ph}(\hbar\omega)W_{ph}(\hbar\omega)d(\hbar\omega)}{\int_0^\infty v_{ph}(\hbar\omega)D_{ph}(\hbar\omega)W_{ph}(\hbar\omega)d(\hbar\omega)} \tag{33}$$

and an average velocity as

$$\left\langle v_{ph}\right\rangle \equiv \frac{\int_0^\infty v_{ph}(\hbar\omega)D_{ph}(\hbar\omega)W_{ph}(\hbar\omega)d(\hbar\omega)}{\int_0^\infty D_{ph}(\hbar\omega)W_{ph}(\hbar\omega)d(\hbar\omega)}\,, \tag{34}$$

with the appropriate averaging.

Equation (17) is often used to estimate the average mean-free-path from the measured κ_L and C_V, if we know the average velocity, which is frequently assumed to be the longitudinal sound velocity. The derivation above has identified the precise definitions of the $\left\langle\left\langle \Lambda_{ph} \right\rangle\right\rangle$ and $\left\langle v_{ph} \right\rangle$. If a phonon dispersion is chosen one can always compute the average velocity according to (34), and it is typically very different from the longitudinal sound velocity. Thus, estimates of the average mean-free-path can be quite wrong if one assumes the longitudinal sound velocity [8].

4. Debye model

For 3D conductors there are three polarization states for lattice vibrations: one for atoms displaced in the direction of propagation (longitudinal/L) and two for atoms displaced orthogonal to the direction of propagation (transverse/T). The low energy modes are called acoustic modes/A: one LA mode analogous to sound waves propagating in air and two TA modes. Near $q \to 0$ dispersion of acoustic modes is linear

$$\hbar\omega = \hbar v_D q\,, \tag{35}$$

and known as Debye approximation. The Debye velocity v_D is an average velocity of the L and T acoustic modes. In case of LA mode v_D is simply the sound velocity $v_s \propto m^{-1/2}$ with m being an effective mass of vibrating atom. Typical $v_s \approx 5\times10^3$ m/s, about 20 times slower that the velocity of a typical electron.

The bandwidth of the electronic dispersion is typically $BW \gg kT$, so only states near the bottom of the conduction band where the effective mass model is reasonably accurate are occupied. For phonons the situation is much different; the bandwidth $BW \approx kT$, so states across the entire Brillouin zone are occupied. The widely-used Debye approximation (35) fits the acoustic branches as long as q is not too far from the center of the Brillouin zone.

With the Debye approximation (35) it is easy to find the density of the phonon states

$$D_{ph}(\hbar\omega) = \frac{3(\hbar\omega)^2}{2\pi^2(\hbar v_D)^3}\,,\ [\mathrm{J}^{-1}\cdot\mathrm{m}^{-3}] \tag{36}$$

where the factor of three is for the three polarizations. Then one can obtain the number of phonon modes per cross-sectional area from eqn (30):

$$M_{ph}(\hbar\omega) = \frac{3(\hbar\omega)^2}{4\pi(\hbar v_D)^2}\,. \tag{37}$$

Since all the states in the Brillouin zone tend to be occupied at moderate temperatures, we are to be sure that we account the correct number of states. For a crystal there are $3N/\Omega$ states per unit volume. To find the total number of states we have to integrate the density-of-states

$$\int_0^{\hbar\omega_D} D_{ph}(\hbar\omega)\, d(\hbar\omega), \tag{38}$$

with the upper limit as $\hbar$ times the so-called Debye frequency to produce the correct number of states, namely:

$$\hbar\omega_D = \hbar v_D \left(\frac{6\pi^2 N}{\Omega} \right)^{1/3} \equiv kT_D . \tag{39}$$

The Debye frequency defines a cutoff frequency above which no states are accounted for. This restriction can also be expressed via a cutoff wavevector q_D or as a Debye temperature

$$T_D = \hbar\omega / k . \tag{40}$$

For $T \ll T_D$ only states with $q \to 0$ for which the Debye approximation is accurate are occupied.

Now we can calculate the lattice thermal conductivity by integrating (11) to the Debye cutoff energy

$$\kappa_L = \frac{\pi^2 k^2 T}{3h} \int_0^{\hbar\omega_D} \frac{M_{ph}(\hbar\omega)}{A} \lambda_{ph}(\hbar\omega) W_{ph}(\hbar\omega)\, d(\hbar\omega) \tag{41}$$

and estimate $M_{ph}(\hbar\omega)$ according to (11). The integral can be taken numerically or analytically if appropriate expression for the mean-free-path is used. This is how the lattice thermal conductivities were first calculated [9, 10]. The theory and computational procedures for the thermoelectric transport coefficients were developed further in [6, 8, 11].

5. Phonon scattering

Phonons can scatter from defects, impurity atoms, isotopes, surfaces and boundaries, electrons, and from other phonons. Phonon-phonon scattering occurs because the potential energy of the bonds in the crystal are not exactly harmonic. All higher order terms are treated as a scattering potential. Two types of phonon scattering are considered. In the normal process two phonons interact and create a third phonon with energy and momentum being conserved:

$$\begin{aligned} \hbar\vec{q}_1 + \hbar\vec{q}_2 &= \hbar\vec{q}_3 \\ \hbar\vec{w}_1 + \hbar\vec{w}_2 &= \hbar\vec{w}_3 \end{aligned} . \tag{42}$$

The total momentum of the phonon ensemble is conserved, thus this type of scattering has little effect on the heat flux.

In a second type of scattering, umklapp/U-scattering the two initial phonons have larger momentum, thus the resulting phonon would have a momentum outside the Brillouin zone due to unharmonic phonon-phonon as well as electron-phonon interactions. The U-scatterings are the basic processes in the heat transport especially at high temperatures. Scattering on defects/D and on boundaries/B are also important. Scattering rates add, thus the total phonon scattering rate is

$$\frac{1}{\tau_{ph}(\hbar\omega)} = \frac{1}{\tau_U(\hbar\omega)} + \frac{1}{\tau_D(\hbar\omega)} + \frac{1}{\tau_B(\hbar\omega)} \tag{43}$$

or alternatively in terms of the mean-free-path (24)

$$\frac{1}{\lambda_{ph}(\hbar\omega)} = \frac{1}{\lambda_U(\hbar\omega)} + \frac{1}{\lambda_D(\hbar\omega)} + \frac{1}{\lambda_B(\hbar\omega)}, \tag{44}$$

Expressions for each of the scattering rates are developed [12]. For scattering from point defects

$$\frac{1}{\tau_D(\hbar\omega)} \propto \omega^4, \tag{45}$$

known as the Rayleigh scattering which is like the scattering of light from the dust.

For boundaries and surfaces

$$\frac{1}{\tau_B(\hbar\omega)} \propto \frac{v_{ph}(\hbar\omega)}{L}, \tag{46}$$

where L is the shortest dimension of the sample.

A commonly used expression for U-scattering is

$$\frac{1}{\tau_U(\hbar\omega)} \propto T^3\omega^2 e^{-T_D/bT}. \tag{47}$$

With this background we are now able to understand the temperature dependence of the lattice thermal conductivity.

6. Lattice thermal conductivity versus temperature

The temperature dependence of the lattice thermal conductivity κ_L is illustrated for bulk *Si* on Fig. 1.

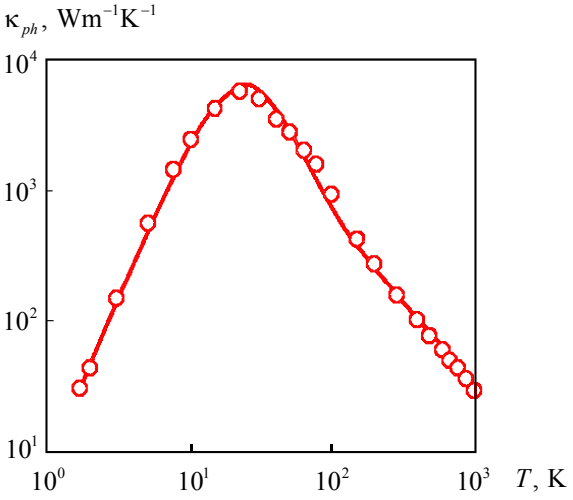

Fig. 1. The experimental [13] and calculated [8] thermal conductivity of bulk Si as a function of temperature.

According to eqn (13) κ_L is proportional to the number of the phonon modes that are occupied $\langle M_{ph} / A \rangle$ and to the average value of the phonon mean-free-path $\langle\langle \lambda_{ph} \rangle\rangle$. The curve $\kappa_L(T)$ can be explained by understanding how $\langle M_{ph} \rangle$ and $\langle\langle \lambda_{ph} \rangle\rangle$ vary with temperature.

It can be shown using eqn (12) that at low temperatures

$$\langle M_{ph} \rangle \propto T^3, \quad (T \to 0) \tag{48}$$

so the initial rise in thermal conductivity is due to the fact that the number of populated modes rises quickly with temperature. At low temperatures boundary scattering is important. As the temperature increases more short-wave-length phonons are produced. These phonons scatter from point defects, so defect scattering becomes more and more important. As the temperature approaches the T_D, all of the phonon modes are populated and further increases in temperature do not change $\langle M_{ph} \rangle$. Instead, the higher temperatures increase the phonon scattering by U-processes, and the thermal conductivity drops with increasing temperatures.

7. Difference between lattice thermal and electrical conductivities

We have already noted the similarity between phonon transport equations (9) and (13) and electron transport equations (15) and (16). The average electron and phonon mean-free-paths are of the same order of magnitude. Why then does the electrical conductance vary over many more orders of magnitude while the lattice thermal conductance varies only over a few? The answer lies in the corresponding windows functions (79) and (81) of [1]. For both electrons and phonons, higher temperatures broaden the window function and increase the population of states. For electrons, however, the position of the Fermi level has a dramatic effect on the magnitude of the window function. By controlling the position of the Fermi level, the electrical conductivity can be varied over many orders magnitude. For the phonons the width of the window function is determined by temperature only.

Another key difference between electrons and phonons relates to how the states are populated. For a thermoelectric device $E_F \approx E_C$, and the electron and phonon window functions are quite similar. However, for electrons the BW of the dispersion is very large, so only a few states near the bottom of the conduction band are populated: the effective mass approximation works well for these states, and it is easy to obtain analytical solutions. For phonons, the BW of the dispersion is small. At moderate temperatures states all across the entire Brillouin zone are occupied: simple analytical approximations do not work, and it is hard to get analytical solutions for the lattice thermal conductivity.

8. Lattice thermal conductivity quantization

By analogy with the electronic conduction quantization

$$G^{ball} = \frac{2q^2}{h} M(E_F), \tag{49}$$

over 30 years ago Pendry [14] stated the existence of the quantum limits to the heat flow. In fact, if $T \to 0$ in eqn (82) of [1] then the phonon window $W_{ph}(\hbar\omega)$ is sharply peaked near $\hbar\omega = 0$:

$$K_L = \frac{\pi^2 k^2 T}{3h} T_{ph}(0) M_{ph}(0). \tag{50}$$

For a bulk conductor $M_{ph}(\hbar\omega) \to 0$ as $\hbar\omega \to 0$, but for a nanoresistors like a nanowire or nanoribbon one can have a finite number of phonon modes. For ballistic phonon transport $T_{ph} = 1$ and one can expect

$$K_L = \frac{\pi^2 k^2 T}{3h} M_{ph}. \tag{51}$$

Exactly this result was proved experimentally using 4-mode resistor at T < 0.8 K [15]; thermoconductivity measurements were agree with the predictions for 1D ballistic resistors [16 – 18].

The quantum of thermal conductance

$$g_0 \equiv \pi^2 k^2 T / 3h \tag{52}$$

represents the maximum possible value of energy transported per phonon mode. Surprisingly, it does not depend on particle statistics: the quantum of thermal conductance is universal for fermions, bosons, and anyons [19 – 21].

Conclusions

As a summary of both papers [1] and the present one we state that the Landauer – Datta – Lundstrom modern electron and heat transport model works well for nano-, micro-, and macroelectronics. If a band structure is chosen analytically or numerically, the number of conduction modes can be evaluated and, if a model for a mean-free-path for backscattering can be established, then the near-equilibrium thermoelectric transport coefficients can be calculated for 1D, 2D, and 3D resistors of any size in ballistic, quasi-ballistic, and diffusive linear response regimes when there are differences in both voltage and temperature across the device.

Finally, we collect below the thermoelectric coefficients through the Fermi – Dirac integrals for parabolic band semiconductors and for graphene in ballistic and diffusive regimes [22].

Appendix A. Thermoelectric coefficients for 1D, 2D, and 3D semiconductors with parabolic dispersion for ballistic and diffusive regimes

Thermoelectric coefficients are expressed through the Fermi – Dirac integral of order *j* defined as

$$\Im_j(\eta_F)=\frac{1}{\Gamma(j+1)}\int_0^\infty\frac{\eta^j}{\exp(\eta-\eta_F)+1}\,d\eta\,,$$

where the location of the Fermi level E_F relative to the conduction band edge E_C is given by the dimensionless parameter

$$\eta_F=\frac{E_F-E_C}{kT}\,.$$

In expressions below thermoelectric coefficients for diffusive regime were calculated with the power law scattering

$$\lambda(E)=\lambda_0\left(\frac{E}{kT}\right)^r.$$

1. Thermoelectric coefficients for 1D ballistic resistors

$$G=\frac{2q^2}{h}\Im_{-1}(\eta_F);\;\; S_T=-\frac{k}{q}\frac{2q^2}{h}\left[\Im_0(\eta_F)-\eta_F\Im_{-1}(\eta_F)\right];\;\; S=-\frac{k}{q}\left[\frac{\Im_0(\eta_F)}{\Im_{-1}(\eta_F)}-\eta_F\right];$$

$$K_0=T\left(\frac{k}{q}\right)^2\frac{2q^2}{h}\left[2\Im_1(\eta_F)-2\eta_F\Im_0(\eta_F)+\eta_F^2\,\Im_{-1}(\eta_F)\right];$$

$$K=T\left(\frac{k}{q}\right)^2\frac{2q^2}{h}\left[2\Im_1(\eta_F)-\frac{\Im_0^2(\eta_F)}{\Im_{-1}(\eta_F)}\right];$$

2. Thermoelectric coefficients for 1D diffusive resistors

$$G=\frac{2q^2}{h}\left(\frac{\lambda_0}{L}\right)\Gamma(r+1)\Im_{r-1}(\eta_F);$$

$$S_T=-\frac{k}{q}\frac{2q^2}{h}\left(\frac{\lambda_0}{L}\right)\Gamma(r+1)\left[(r+1)\Im_r(\eta_F)-\eta_F\Im_{r-1}(\eta_F)\right];\; S=-\frac{k}{q}\left[\frac{(r+1)\Im_r(\eta_F)}{\Im_{r-1}(\eta_F)}-\eta_F\right];$$

$$K_0=T\left(\frac{k}{q}\right)^2\frac{2q^2}{h}\left(\frac{\lambda_0}{L}\right)\left[\Gamma(r+3)\Im_{r+1}(\eta_F)-2\eta_F\Gamma(r+2)\Im_r(\eta_F)+\eta_F^2\Gamma(r+1)\Im_{r-1}(\eta_F)\right];$$

$$K=T\left(\frac{k}{q}\right)^2\frac{2q^2}{h}\left(\frac{\lambda_0}{L}\right)\Gamma(r+2)\left[(r+2)\Im_{r+1}(\eta_F)-\frac{(r+1)\Im_r^2(\eta_F)}{\Im_{r-1}(\eta_F)}\right];$$

Conductivity $G=\sigma_{1D}/L$ is given in Siemens: $\left[\sigma_{1D}\right]=1\,\mathrm{S}\cdot\mathrm{m}$. Similarly for other specific coefficients: $s_T=S_TL;\quad \kappa_0=K_0L;\quad \kappa=KL.$

3. Thermoelectric coefficients for 2D ballistic resistors

$$G=W\frac{2q^2}{h}\frac{\sqrt{2\pi m^*kT}}{h}\Im_{-1/2}(\eta_F);$$

$$S_T=-W\frac{k}{q}\frac{2q^2}{h}\frac{\sqrt{2\pi m^*kT}}{h}\left[\frac{3}{2}\Im_{1/2}(\eta_F)-\eta_F\Im_{-1/2}(\eta_F)\right];\;\; S=-\frac{k}{q}\left[\frac{3\Im_{1/2}(\eta_F)}{2\Im_{-1/2}(\eta_F)}-\eta_F\right];$$

$$K_0 = W\,T\left(\frac{k}{q}\right)^2 \frac{2q^2}{h}\frac{\sqrt{2\pi m^* kT}}{h}\left[\frac{15}{4}\Im_{3/2}(\eta_F) - 3\eta_F\Im_{1/2}(\eta_F) + \eta_F^2\Im_{-1/2}(\eta_F)\right];$$

$$K = W\,T\left(\frac{k}{q}\right)^2 \frac{2q^2}{h}\frac{\sqrt{2\pi m^* kT}}{h}\left[\frac{15}{4}\Im_{3/2}(\eta_F) - \frac{9\Im_{1/2}^2(\eta_F)}{4\Im_{-1/2}(\eta_F)}\right];$$

4. Thermoelectric coefficients for 2D diffusive resistors

$$G = W\frac{2q^2}{h}\left(\frac{\lambda_0}{L}\right)\frac{\sqrt{2m^* kT}}{\pi h}\Gamma(r+\frac{3}{2})\Im_{r-1/2}(\eta_F);\;\; S = -\frac{k}{q}\left[\frac{(r+3/2)\Im_{r+1/2}(\eta_F)}{\Im_{r-1/2}(\eta_F)} - \eta_F\right];$$

$$S_T = -W\frac{k}{q}\frac{2q^2}{h}\left(\frac{\lambda_0}{L}\right)\frac{\sqrt{2m^* kT}}{\pi h}\left[\Gamma(r+\frac{5}{2})\Im_{r+1/2}(\eta_F) - \eta_F\Gamma(r+\frac{3}{2})\Im_{r-1/2}(\eta_F)\right];$$

$$K_0 = W\,T\left(\frac{k}{q}\right)^2 \frac{2q^2}{h}\left(\frac{\lambda_0}{L}\right)\frac{\sqrt{2m^* kT}}{\pi h}\times$$
$$\times\left[\Gamma(r+\frac{7}{2})\Im_{r+3/2}(\eta_F) - 2\eta_F\Gamma(r+\frac{5}{2})\Im_{r+1/2}(\eta_F) + \eta_F^2\Gamma(r+\frac{3}{2})\Im_{r-1/2}(\eta_F)\right];$$

$$K = W\,T\left(\frac{k}{q}\right)^2 \frac{2q^2}{h}\left(\frac{\lambda_0}{L}\right)\frac{\sqrt{2m^* kT}}{\pi h}\Gamma(r+\frac{5}{2})\left[(r+\frac{5}{2})\Im_{r+3/2}(\eta_F) - \frac{(r+\frac{3}{2})\Im_{r+1/2}^2(\eta_F)}{\Im_{r-1/2}(\eta_F)}\right];$$

Conductivity $G = \sigma_{2D}W/L$ is given in Siemens: $[\sigma_{2D}] = 1\,\mathrm{S}$. Similarly for other specific coefficients: $s_T = S_T L/W;\quad \kappa_0 = K_0 L/W;\quad \kappa = KL/W.$

5. Thermoelectric coefficients for 3D ballistic resistors

$$G = A\frac{2q^2}{h}\frac{m^* kT}{2\pi\hbar^2}\Im_0(\eta_F);\;\; S_T = -A\frac{k}{q}\frac{2q^2}{h}\frac{m^* kT}{2\pi\hbar^2}\left[2\Im_1(\eta_F) - \eta_F\Im_0(\eta_F)\right];\;\; S = -\frac{k}{q}\left[\frac{2\Im_1(\eta_F)}{\Im_0(\eta_F)} - \eta_F\right];$$

$$K_0 = AT\left(\frac{k}{q}\right)^2 \frac{2q^2}{h}\frac{m^* kT}{2\pi\hbar^2}\left[6\Im_2(\eta_F) - 4\eta_F\Im_1(\eta_F) + \eta_F^2\Im_0(\eta_F)\right];$$

$$K = AT\left(\frac{k}{q}\right)^2 \frac{2q^2}{h}\frac{m^* kT}{2\pi\hbar^2}\left[6\Im_2(\eta_F) - \frac{4\Im_1^2(\eta_F)}{\Im_0(\eta_F)}\right];$$

6. Thermoelectric coefficients for 3D diffusive resistors

$$G = A\frac{2q^2}{h}\left(\frac{\lambda_0}{L}\right)\frac{m^* kT}{2\pi\hbar^2}\Gamma(r+2)\Im_r(\eta_F);\;\; S = -\frac{k}{q}\left[\frac{(r+2)\Im_{r+1}(\eta_F)}{\Im_r(\eta_F)} - \eta_F\right];$$

$$S_T = -A\frac{k}{q}\frac{2q^2}{h}\left(\frac{\lambda_0}{L}\right)\frac{m^* kT}{2\pi\hbar^2}\left[\Gamma(r+3)\Im_{r+1}(\eta_F) - \eta_F\Gamma(r+2)\Im_r(\eta_F)\right];$$

$$K_0 = AT\left(\frac{k}{q}\right)^2 \frac{2q^2}{h}\left(\frac{\lambda_0}{L}\right)\frac{m^* kT}{2\pi\hbar^2}\left[\Gamma(r+4)\Im_{r+2}(\eta_F) - 2\eta_F\Gamma(r+3)\Im_{r+1}(\eta_F) + \eta_F^2\Gamma(r+2)\Im_r(\eta_F)\right];$$

$$K = AT\left(\frac{k}{q}\right)^2 \frac{2q^2}{h}\left(\frac{\lambda_0}{L}\right)\frac{m^* kT}{2\pi\hbar^2}\Gamma(r+3)\left[(r+3)\Im_{r+2}(\eta_F) - \frac{(r+2)\Im_{r+1}^2(\eta_F)}{\Im_r(\eta_F)}\right];$$

Conductivity $G = \sigma_{3D} A / L$ is given in Siemens: $[\sigma_{3D}] = 1$ S/m. Similarly for other specific coefficients: $s_T = S_T L / A; \quad \kappa_0 = K_0 L / A; \quad \kappa = KL / A.$

Appendix B. Thermoelectric coefficients for graphene with linear dispersion for ballistic and diffusive regimes

Graphene is a 2D conductor with a unique linear band structure $E(k) = \pm\hbar v_F k$. Its transport coefficients are calculated from eqs (65) and (67) of [1] with the number of modes given by $M(E) = W \cdot 2|E|/\pi\hbar v_F$. The power law scattering for diffusive regime is used as above.

Conductivity $G = \sigma W / L$ is given in Siemens: $[\sigma] = 1$ S. Similarly for other specific coefficients: $s_T = S_T L / W; \ \kappa_0 = K_0 L / W; \ \kappa = K L / W.$

1. Ballistic regime

$$G^{ball} = W\frac{2q^2}{h}\left(\frac{2kT}{\pi\hbar v_F}\right)\left[\Im_0(\eta_F) + \Im_0(-\eta_F)\right]; \ S^{ball} = -\frac{k}{q}\left\{\frac{2\left[\Im_1(\eta_F) - \Im_1(-\eta_F)\right]}{\Im_0(\eta_F) + \Im_0(-\eta_F)} - \eta_F\right\};$$

$$S_T^{ball} = -W\frac{2q^2}{h}\left(\frac{2kT}{\pi\hbar v_F}\right)\left(\frac{k}{q}\right)\left\{2\left[\Im_1(\eta_F) - \Im_1(-\eta_F)\right] - \eta_F\left[\Im_0(\eta_F) + \Im_0(-\eta_F)\right]\right\};$$

$$K^{ball} = WT\frac{2q^2}{h}\left(\frac{2kT}{\pi\hbar v_F}\right)\left(\frac{k}{q}\right)^2\left\{6\left[\Im_2(\eta_F) + \Im_2(-\eta_F)\right] - \frac{4\left[\Im_1(\eta_F) - \Im_1(-\eta_F)\right]^2}{\Im_0(\eta_F) + \Im_0(-\eta_F)}\right\};$$

$$K_0^{ball} = WT\frac{2q^2}{h}\left(\frac{2kT}{\pi\hbar v_F}\right)\left(\frac{k}{q}\right)^2 \times$$
$$\times\left\{6\left[\Im_2(\eta_F) + \Im_2(-\eta_F)\right] - 4\eta_F\left[\Im_1(\eta_F) - \Im_1(-\eta_F)\right] + \eta_F^2\left[\Im_0(\eta_F) + \Im_0(-\eta_F)\right]\right\}.$$

2. Diffusive regime

$$G^{diff} = W\frac{2q^2}{h}\left(\frac{2kT}{\pi\hbar v_F}\right)\left(\frac{\lambda_0}{L}\right)\Gamma(r+2)\left[\Im_r(\eta_F) + \Im_r(-\eta_F)\right];$$

$$S^{diff} = -\frac{k}{q}\left\{\frac{(r+2)\left[\Im_{r+1}(\eta_F) - \Im_{r+1}(-\eta_F)\right]}{\Im_r(\eta_F) + \Im_r(-\eta_F)} - \eta_F\right\};$$

$$S_T^{diff} = -W\frac{2q^2}{h}\frac{k}{q}\left(\frac{2kT}{\pi\hbar v_F}\right)\left(\frac{\lambda_0}{L}\right)\left\{\begin{matrix}\Gamma(r+3)\left[\Im_{r+1}(\eta_F) - \Im_{r+1}(-\eta_F)\right] - \\ -\eta_F\Gamma(r+2)\left[\Im_r(\eta_F) + \Im_r(-\eta_F)\right]\end{matrix}\right\};$$

$$K = W\,T\,\frac{2q^2}{h}\left(\frac{k}{q}\right)^2\left(\frac{2kT}{\pi\hbar v_F}\right)\left(\frac{\lambda_0}{L}\right)\times$$
$$\times\Gamma(r+3)\left\{(r+3)\left[\Im_{r+2}(\eta_F)+\Im_{r+2}(-\eta_F)\right]-\frac{(r+2)\left[\Im_{r+1}(\eta_F)-\Im_{r+1}(-\eta_F)\right]^2}{\Im_r(\eta_F)+\Im_r(-\eta_F)}\right\};$$

$$K_0 = W\,T\,\frac{2q^2}{h}\left(\frac{k}{q}\right)^2\left(\frac{2kT}{\pi\hbar v_F}\right)\left(\frac{\lambda_0}{L}\right)\times$$
$$\times\left\{\begin{array}{l}\Gamma(r+4)\left[\Im_{r+2}(\eta_F)+\Im_{r+2}(-\eta_F)\right]-2\eta_F\Gamma(r+3)\left[\Im_{r+1}(\eta_F)+\Im_{r+1}(-\eta_F)\right]+\\ +\eta_F^2\Gamma(r+2)\left[\Im_r(\eta_F)+\Im_r(-\eta_F)\right]\end{array}\right\}.$$

References

1. Yu. A. Kruglyak, *J. Thermoelecticity*, N X, XXX (2014).
2. J. M. Ziman, *Principles of the Theory of Solids* (Cambridge Univercity Press, Cambridge, 1964).
3. C. Kittel, *Introduction to Solid State Physics* (John Wiley and Sons, New York, 1971).
4. N. W. Ashcroft and N.D. Mermin, *Solid State Physics* (Saunders College, Philadelphia, 1976).
5. L. I. Anatychuk, *Thermoelectricity. V. 1. Physics of Thermoelectricity* (Bookrek, Chernivtsi, 2009).
6. C. Jeong, R. Kim, M. Luisier, S. Datta, and M. Lundstrom, *J. Appl. Phys*. **107**, 023707 (2010).
7. M. Lundstrom, *Fundamentals of Carrier Transport* (Cambridge University Press, Cambridge, 2012).
8. C. Jeong, S. Datta, and M. Lundstrom, *J. Appl. Phys*. **109**, 073718 (2011).
9. J. Callaway, *Phys. Rev*. **113**, 1046 (1959).
10. M. G. Holland, *Phys. Rev*. **132**, 2461 (1963).
11. C. Jeong, S. Datta, and M. Lundstrom, *J. Appl. Phys*. **111**, 093708 (2012).
12. C. Gang, *Nanoscale Energy Transport and Conversion: A Parallel Treatment of Electrons, Molecules, Phonons, and Photons* (Oxford University Press, New York, 2005).
13. C. J. Glassbrenner and G.A. Slack, *Phys. Rev. A*, **134**, 1058 (1964).
14. J. B. Pendry, *J. Phys. A*, **16**, 2161 (1983).
15. K. Schwab, E.A. Henriksen, J.M. Worlock, and M.L. Roukes, *Nature*, **404**, 974 (2000).
16. D. E. Angelescu, M.C. Cross, and M.L. Roukes, *Superlatt. Microstruct*. **23**, 673 (1998).
17. L. G. C. Rego, and G. Kirczenow, *Phys. Rev. Lett*. **81**, 232 (1998).
18. M. P. Blencowe, *Phys. Rev. B*, **59**, 4992 (1999).
19. L. G. C. Rego, and G. Kirczenow, *Phys. Rev. B*, **59**, 13080 (1999).
20. I. V. Krive, and E.R. Mucciolo, *Phys. Rev. B*, **60**, 1429 (1999).
21. C. M. Caves, and P.D. Drummond, *Rev. Mod. Phys*. **66**, 481 (1994).
22. R. S. Kim, *Physics and simulation of Nanoscale Electronic and Thermoelectric Devices* (Purdue University, West Lafayette, 2011).

Submitted 21.11.2014